CALT-68-2749

LHC Searches for Non-Chiral Weakly Charged Multiplets

Matthew R. Buckley[1], Lisa Randall[2], and Brian Shuve[2]
[1]*Department of Physics, California Institute of Technology, Pasadena, CA 91125, USA and*
[2]*Harvard University, Cambridge, MA 02138, USA*
(Dated: September 24, 2009)

Because the TeV-scale to be probed at the Large Hadron Collider should shed light on the naturalness, hierarchy, and dark matter problems, most searches to date have focused on new physics signatures motivated by possible solutions to these puzzles. In this paper, we consider some candidates for new states that although not well-motivated from this standpoint are obvious possibilities that current search strategies would miss. In particular we consider vector representations of fermions in multiplets of $SU(2)_L$ with a lightest neutral state. Standard search strategies would fail to find such particles because of the expected small one-loop-level splitting between charged and neutral states.

I. INTRODUCTION

Based on the Higgs mechanism and the hierarchy problem, we expect new physical states to be produced at the TeV scale. Current LHC strategies focus on discovery of different models that address these problems, such as supersymmetry (SUSY) [1], extra dimensions [2, 3] and technicolor [4, 5, 6].

However, other states may appear at the TeV scale that are irrelevant to the working of the Higgs mechanism or solutions to the hierarchy problem but might nonetheless be part of a TeV-sector. An obvious example would be states that are nonchiral under electroweak gauge symmetry. Such states can be motivated in specific theories – as dark matter candidates [7, 8, 9], or to relax constraints from electro-weak symmetry breaking (EWSB) [10]. In this paper we will not assume any specific model-building goal but assume only that as with dark matter candidates, the lightest state in the multiplets is neutral.

In particular, we consider new vector-like fermions in multiplets of $SU(2)_L$ where the splitting between the charged and neutral states is due solely to loop corrections, which will generally be the case unless there are special additional interactions. As a consequence, the spectrum in these theories is nearly degenerate; only a few hundred MeV separate the states.

Remarkably, current searches would not find such multiplets, even if they are as light as 100 GeV. This surprising fact is the result of the small one-loop splittings, which imply final states with very soft Standard Model (SM) fields and an invisible uncharged heavy particle. The charged states decay rapidly into the neutral particle and light SM fields (typically electrons, neutrinos, or pions) while the neutral states (which may or may not be a viable thermal DM candidates) are stable and so escape undetected. The physical distance traveled by the charged state depends strongly on the splitting ΔM; it is on the order of 10 meters when $\Delta M < m_\pi$, dropping to ~ 10 cm once the two-body pion channel opens up ($\Delta M \gtrsim m_\pi$), and falling rapidly for larger mass splittings.

Current search strategies for new long-lived particles rely on looking for charged states that make it all the way through the detector [11, 12]. Such searches will not find the vector multiplets we are considering; they would find only those multiplets that contain exclusively charged states or those that have $\Delta M < m_\pi$, and thus a lifetime long enough to reach the muon chamber. However, if the lightest state in the multiplet is neutral and the splitting is bigger, the detector would register only short 'stub' tracks from the charged states. This means that, even if these particles can be produced at reasonably large rates, standard searches would miss them.

The case of $SU(2)_L$ triplet scalars has been investigated in Ref. [10]. Such models have similar splittings and couplings, and so have a great deal of collider phenomenology in common with the fermion case considered in this paper. These scalar fields will also in the most general case have tree-level couplings to the Higgs, which could be used to distinguish between the scalar and fermionic models.

Wino lightest supersymmetric particles (LSPs) that are nearly degenerate with a charged next-to-lightest supersymmetric particle (NLSP) are an example of a 'complete' model which has similar phenomenology to the simple vector multiplets. As a result, the experimental considerations are closely related [13, 14, 15, 16]. Such a SUSY spectrum occurs in anomaly-mediated supersymmetry breaking [18, 19], when either $|\mu| \gg M_1 > M_2$ or $M_{1/2} \gg |\mu|$. In both situations, the LSP is the neutralino $\tilde{\chi}_1^0$ and the next-to-lightest supersymmetric particle (NLSP) is the chargino $\tilde{\chi}_1^\pm$. In the former case both are primarily wino. In this limit the tree-level splitting is suppressed by $|\mu|^2$, and is commensurate with the loop splitting common to all $SU(2)_L$ triplets. The latter case (small $|\mu|$) is very similar, though here the LSP and NLSP are primarily higgsino. Since only the LSP and NLSP would typically be accessible in these scenarios, searches for such spectra has long been recognized as extremely challenging. Proposals for search strategies have been made for the Tevatron [13, 14], the LHC [15], and been carried out at DELPHI [16] and OPAL

[17]. As this phenomenology is essentially an example of a generic degenerate multiplet, the search proposed here overlaps with this body of previous work. It is important to recognize that those searches have potentially greater applicability than just anomaly-mediated supersymmetry breaking.

The searches we consider in this paper would be quite worthwhile in that current bounds on such states are pitifully weak. New particles coupling to the Z boson must be heavier than $m_Z/2$ [21]. The LEP-II search by DELPHI [16] placed a lower bound on degenerate winos of approximately 90 GeV for mass splittings less then ~ 200 MeV. OPAL excluded a 95 GeV higgsino- or wino-like LSP/NLSP pair with splittings larger than 0.5 GeV [17]. The limits are relaxed to $50 - 60$ GeV for GeV-scale splittings.

Several additional proposals have been made for alternative searches at colliders in current operation. However, these have not yet been implemented. For splittings between $300 - 600$ MeV, the Tevatron might be able to place limits between 68(95) and 53(75) GeV with an integrated luminosity of 2(30) fb^{-1} using searches for short 'stubs' of the kind investigated in this paper, combined with other techniques for longer tracks [14]. The LEP-II doublet search proposed by Thomas and Wells [22] would be sensitive to 70 GeV masses, with splittings on the order of 300 MeV. As a linear collider is free of large low-energy hadronic background from the underlying event, these authors proposed a search for soft pions from the charged particle's displaced vertex. As with the Tevatron proposal, this search has also not been performed.

Given the weakness of current bounds, any improvement would be worthwhile. Surprisingly, the only significant bound improvements are likely to be on triplet states although with enough luminosity some improvement on bounds for other multiplets might be possible. We will show that we might extend the mass reach for vector-like triplets to 500 GeV under optimistic high-luminosity LHC scenarios, and that even in early running the bounds can be significantly improved.

We now briefly outline the experimental issues and our proposed strategy. Due to the relatively rapid decay (compared to the length scales of the detector) of the charged states ($X^\pm$) to the invisible lighter neutral state (X^0) plus very low energy pions or electrons, experimental detection is extremely difficult. When rapid decay to pions dominates ($\Delta M > m_\pi$), pair production of $X^\pm X^\mp + X^\pm X^0$ is effectively invisible, since there is not a large amount of energy deposited in any calorimeter layer or the muon system. Due to the lack of energy deposition, such events are not triggered upon and so would not even be written to tape. Smaller splittings ($\Delta M < m_\pi$) would be less troublesome, as the longer lifetime resulting from phase space suppression to $X^0 e^\pm \nu_e$ states allows the $X^\pm$ to pass through the calorimeter and even the muon system, appearing as a slow, heavy, massive charged particle as it does so [14]. We will focus on the more difficult short track search in this paper.

When the splitting is large enough to permit the pion decay mode, associated production of either photons or jets at high p_T will be needed to pass the detector trigger. Comparing the two processes at the LHC, only jets would yield sufficient rate. One can trigger on either high p_T jets or on missing transverse energy (MET) (or on both), where the missing E_T comes from a pair of X particles recoiling against one or more jets. Once the events are triggered on and recorded, off-line analysis will be used to look for the short charged state tracks (prior to decay).

If the mass splitting is close to the pion mass, the typical $c\tau$ of the charged particles is on the order of 10 cm. The central trackers of both CMS and ATLAS consist of multiple detector layers spaced ~ 5 cm to ~ 50 cm from the beam pipe. For this range of mass parameters, the charged track may be reconstructed off-line by requiring ≥ 3 hits in the silicon tracker, with the main background presumably being the combinatoric one from hits that accidentally line up. Specialized reconstruction techniques would be required since current algorithms require energy deposition in the calorimeters or muon system to confirm a track. Using both charged-charged and charged-neutral production and studying relative rates could help reduce the background.

For larger splittings, 200 MeV $\lesssim \Delta M \lesssim 1$ GeV, the decay length is $\lesssim 1$ cm so the tracks would be too short to reliably affect even one layer of the detector. While the pions in this case may have high enough transverse energy (E_T) to be efficiently detected, the huge hadronic background present in every bunch-crossing at the LHC completely dwarfs any possible signal. Detection of such particles would be possible only at lower masses (and thus higher production cross sections) as the number of long lifetime events reaching three or more layers is exponentially suppressed.

In Section II we outline the models and spectra used in the remainder of the paper. We consider new $SU(2)_L$ triplets and new $SU(2)_L$ doublets, the phenomenology of which is detailed in Section III. These simple models are highly predictive and suggest important qualitative and quantitative differences in the strategy for discovery at the LHC. Perturbations on these simple models (including the case of anomaly mediated winos) will be discussed in Section IV.

II. MODELS

As stated in the introduction, in this paper we are not attempting to create a full model of TeV-scale physics that addresses the known issues with the Standard Model: electroweak symmetry breaking (EWSB), dark matter, naturalness and the hierarchy problem. Rather, we take a minimalist approach, introducing vector fermions charged under $SU(2)_L$ (with appropriate hypercharge to have a neutral component) and investigating the reach of the LHC in discovering such particles. It is interesting that what amounts to heavy vector-representation leptons are so difficult to detect.

The Lagrangian of our minimal model consists of just the standard kinetic and mass terms:

$$\mathcal{L} = i\bar{X}\not{D}X - M\bar{X}X. \tag{1}$$

Here the X fields are vector fermions (that is, both left- and right-handed components have the same quantum numbers) in a multiplet $m = 2, 3, \ldots$ of $SU(2)_L$. We are interested in the cases where one of the components of the multiplet has $Q_{\rm EM} = 0$ after electroweak symmetry breaking. This limits the choices of hypercharge Y; for $m = 2$, $Y = \pm 1/2$, $m = 3$, $Y = 0, \pm 1$; *etc.* For specificity and because they are sufficient to illustrate qualitatively different detector phenomenology, we choose to consider two cases: $m = 2$, $Y = 1/2$ doublets X_2, and $m = 3$, $Y = 0$ triplets X_3. We will, however, comment briefly on the phenomenology of other possibilities in this section.

For doublets there are four degrees of freedom:

$$X_2 = \begin{pmatrix} X_2^+ \\ X_2^0 \end{pmatrix}\ ,\ \bar{X}_2 = \begin{pmatrix} \bar{X}_2^0 \\ X_2^- \end{pmatrix}. \tag{2}$$

We choose triplets in a real representation of $SU(2)_L$. This requires only three degrees of freedom:

$$X_3 = \begin{pmatrix} X_3^+ \\ X_3^0 \\ X_3^- \end{pmatrix}. \tag{3}$$

Notice that we could equally well have chosen six degrees of freedom for the triplets (by introducing an $\bar{X}_3$). However, later we will draw connections between the triplet model and anomaly-mediated winos, so we choose to focus on the Majorana case. In all cases, the particle representations are vector-like and so the new states do not contribute to anomalies.

With the Lagrangian of Eq. (1), all components of the X multiplet are degenerate at tree level. Splittings between the charged and neutral components arise from loops of the W^3 gauge boson (or Z/γ loops after EWSB). The mass splitting ΔM between the state with charge Q and the neutral state is [8]

$$\Delta M = \frac{\alpha M}{4\pi}\left\{Q^2 f\left(\frac{M_Z}{M}\right) + \frac{Q(Q-2Y)}{\sin^2\theta_W}\left[f\left(\frac{M_W}{M}\right) - f\left(\frac{M_Z}{M}\right)\right]\right\}, \tag{4}$$

where the function f is

$$f(x) = \frac{x}{2}\left[2x^3\ln x - 2x + \sqrt{x^2-4}(x^2+2)\ln(x^2 - 2 - x\sqrt{x^2-4})/2\right]. \tag{5}$$

The resulting mass splittings $\Delta M(M)$ between the charged and neutral states for the doublets X_2 and triplets X_3 are displayed in Fig. 1.

These mass splittings have several features of interest. As expected, the scale of ΔM is down from M by a loop factor $\alpha/4\pi$, leading to $\mathcal{O}(100$ MeV) splittings from TeV-scale masses. This has important consequences for the decay width of $X^\pm \to X^0 +$ (SM fields).

The electron mode dominates for $\Delta M < m_\pi$, but once kinematically allowed, the single pion mode dominates until $\Delta M \gtrsim 1$ GeV [23]. Beyond this splitting, the $\pi^\pm\pi^0$ and other hadronic modes become important. As can be seen from Fig. 1, the scale of ΔM is about 300 MeV for doublets and approximately 150 MeV for triplets allowing us to ignore all modes except the single pion (Eq. (6)). Since $\Delta M \sim \Lambda_{\rm QCD}$, only the two-body channel $X^\pm \to X^0\pi^\pm$ is open, and two-body kinematics causes this mode to dominate for this range of mass splittings.

A perhaps counter-intuitive result of Eq. (4) is that the splitting of the triplets is smaller than that of the doublet. This is because of the non-zero hypercharge required for a neutral component of the X_2 multiplet. Since the splitting is smaller for X_3 and is only marginally larger than m_π, the triplet lifetime is much longer than that of X_2.

From Eq. (4), we find a generic result for vector fermions in a representation m of $SU(2)_L$ with a neutral ground state. The $X^\pm - X^0$ splittings for even m will be $\mathcal{O}(300$ MeV) for $M \gtrsim 200$ GeV, while for odd m, ΔM will be

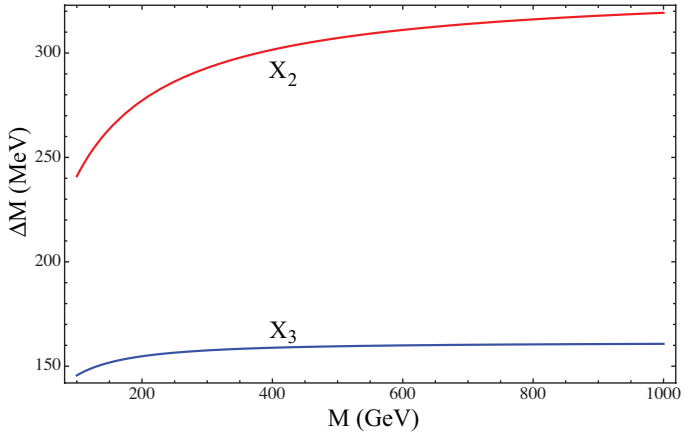

FIG. 1: Splittings between the charged $X^\pm$ and neutral X^0 states for $SU(2)_L$ doublets X_2 (red line) and triplets X_3 (blue) as a function of neutral state mass M.

$\mathcal{O}(150$ MeV), assuming $Y = 0$. Of course, when $Y \neq 0$, the odd m splittings will generally be larger than that of the even representations.

The $X^\pm$ decay widths into various final states have been calculated in several sources for doublets [22], triplets [15, 23], and higher multiplets [8]. The most relevant for our purposes are the decays to a single pion or $\ell\nu_\ell$ pair, which have widths of

$$\Gamma(X^\pm \to X^0\pi^\pm) = \frac{AG_F^2}{4\pi}\cos^2\theta_c f_\pi^2 \Delta M^3 \sqrt{1-\frac{m_\pi^2}{\Delta M^2}} \tag{6}$$

$$\Gamma(X^\pm \to X^0\ell^\pm\nu_\ell) = \frac{AG_F^2}{60\pi^3}\Delta M^5 \sqrt{1-\frac{m_\ell^2}{\Delta M^2}} P\left(\frac{m_\ell}{\Delta M}\right), \tag{7}$$

where $f_\pi \approx 130$ MeV is the pion decay constant, θ_c is the Cabibbo angle, $A = m^2$ for even representations m of $SU(2)_L$, for odd representations $A = 4(m^2-1)$, and the function $P(x)$ is defined as

$$P(x) = 1 - \frac{9}{2}x^2 - 4x^4 + \frac{15x^4}{2\sqrt{1-x^2}}\tanh^{-1}\sqrt{1-x^2}. \tag{8}$$

The resulting lifetime $c\tau$ for a multiplet with splitting ΔM is shown in Fig. 2(a), while the lifetime of the doublets and triplets as a function of the X^0 mass M is shown in Fig. 2(b). As expected, there is a noticeable 'kink' structure when the pion channel opens at $\Delta M = m_\pi$. For $X_2^0(X_3^0)$ masses above 200 GeV, the lifetime is remarkably constant at $\sim 1(10)$ cm.

When viewing $c\tau$ keep in mind that this is not the physical distance that will be measured in the detector. When the factors $\beta\gamma$ are included, the path lengths generally increase by a factor of a few. However, since only the transverse distance is relevant to track determination, the physically relevant distance will be comparable to the $c\tau$ values presented below. These numbers will be made more precise when we consider actual event simulations.

The simple Lagrangian of Eq. (1) provides a very predictive model for experimental searches. Charged particles will be created (either in pairs or in conjunction with a neutral state), travel $\mathcal{O}(10$ cm) for triplets or $\mathcal{O}(1$ cm) for doublets, and decay into an invisible X^0 and a very low energy pion. A new vector triplet with mass of $\mathcal{O}$(TeV) would have a mass splitting between the X_3^+ and X_3^0 states that is only slightly above the pion mass. From the point of view of an LHC experiment (ATLAS or CMS), the X_3^+ (in principle visible as an ionizing charged track in the central tracker), will decay into an invisible X_3^0 and a pion after $\mathcal{O}(10$ cm).

In the rest frame of the decaying particle, the energy of this outgoing pion is

$$E_\pi = \frac{2M\Delta M + \Delta M^2 + m_\pi^2}{2(M+\Delta M)} \sim \Delta M \sim 150 \text{ MeV}. \tag{9}$$

The experimentally relevant parameter is not E_π, but the transverse pion energy E_T, which is of course smaller. While we may expect some gain in available energy due to relativistic boosts of the parent particle, this is not significant for the range of M we are interested in. For these ranges of E_T, the pions will typically not even register in the detector. Therefore the search strategy in this case will be to look for stubs from charged tracks after triggering on missing or jet energy.

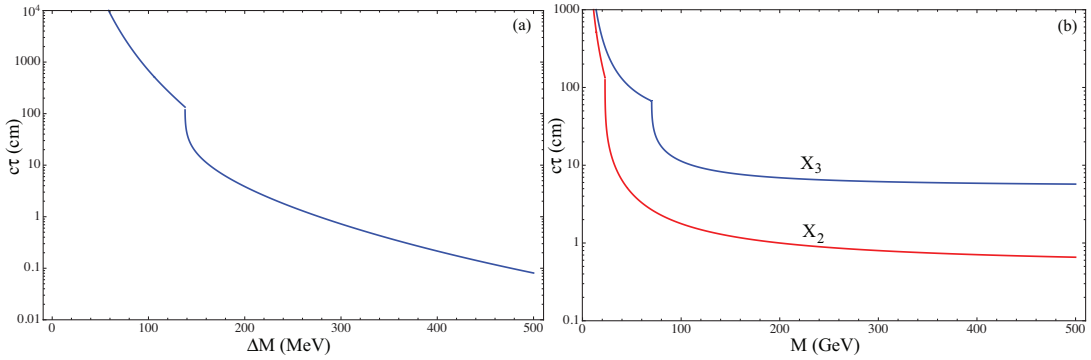

FIG. 2: Left: Lifetime of generic $X^\pm$ decaying to the final states $X^0 + \pi^\pm$ or $X^0 + \ell^\pm + \nu_\ell$ as a function of $X^\pm - X^0$ mass splitting ΔM. Here $\ell = e/\mu$. We have assumed that the X couples to $W^\pm$ with the same strength as a triplet (*i.e.* $A = 8$ in Eqs. (6) and (7) The 'kink' structure at $\Delta M = m_\pi$ is caused by the pion channel opening. Right: Lifetime of doublets $X_2^\pm$ and triplets $X_3^\pm$ decaying to the neutral states X_2^0/X_3^0 as a function of the neutral state mass M, assuming the mass splittings of Eq. (4).

Doublets on the other hand generally have larger splittings. This implies the lifetime and track stub length is expected to be shorter than that of triplets, making the search for stubs even more challenging. The pion transverse momentum is generally bigger, in the range of efficient detection at ATLAS and CMS [24]. However, even though the pions from these decays will be isolated from jets and have large impact parameters, the extremely large background of pions from the underlying event (and pile-up during high luminosity runs) will almost certainly make such detection impossible.

For larger splittings on the order of 1 GeV, the decay mode includes multiple pions and other hadronic states. Jets with E_T on the order of a GeV and large impact parameters are a key part of b-jet tagging [25]. Thus, once $\Delta M \sim \mathcal{O}(1\text{ GeV})$, standard triggers should be capable of registering their presence. Models with such large splittings are not considered in this paper. However, we note that this nonetheless leaves a range of ΔM from ~ 200 MeV to 1 GeV where detection of new multiplets is extremely unlikely.

Although generically the relation Eq. (4) holds, there are important exceptions. In Section IV we will also consider an interpolating scenario between that of the doublets and the triplets where M and ΔM are less rigidly connected than in Eq. (4). This is important since the key parameter for all these searches is the splitting ΔM, which controls the branching ratios, lifetimes, and energies of the final states in the detectors.

As we shall see, the charged particle width Γ essentially determines the detectability of a model. This parameter is set by a combination of the splitting and the couplings to $W^\pm$ (see Eq. (6)). While the splitting for higher odd multiplets remains small (for zero hypercharge), the larger couplings increase Γ and thus make those scenarios more difficult to discover, though we would be aided by the larger production cross section.

As an explicit example, consider an $m = 5$ multiplet with zero hypercharge. This consists of neutral, $\pm e$ and $\pm 2e$ charged states. The splitting between the neutral and singly charged states is the same as in the $m = 3$ triplet, while the doubly charged states are ~ 650 MeV heavier than the X_5^0. These doubly charged $X_5^{\pm\pm}$ states would rapidly decay first to $X_5^\pm$ and then to the neutral state. Due to smallness of the mass splitting and resulting low energy of the SM decay products, it is unlikely that the byproducts of such a cascade would be visible at the LHC, or that the heavy charged particle would be deflected by a noticeable amount. This makes the $X_5^{\pm\pm}$ production act effectively as an increase in the $X_5^\pm$ production cross section. The $X_5^\pm$ then decays to $X_5^0\pi^\pm$ more quickly than an equal mass $X_3^\pm$, due to the larger coupling of higher multiplets to $W^\pm$. For a generic odd multiplet m, the width goes as $m^2 - 1$, while for even m widths are proportional to m^2.

As a result, an $m = 5$ multiplet would decay faster than a triplet by a factor of eight. The detector phenomenology would be similar to that of the doublet but with a larger apparent production of singly charged heavy states and slightly longer tracks.[1] Surprisingly, triplets are therefore the easiest multiplet to discover, as they have the longest decay length. Below we consider both triplets and doublets, the latter of which can still have an improved bound over current constraints, even with their larger mass splitting.

[1] A future linear collider, free of the large hadronic background from the underlying event, might be able to find the pions from cascade decays of high multiplets. Such a search is beyond the scope of this paper.

III. SIGNATURE OF TRIPLETS AND DOUBLETS

As we've seen, the small pion E_T is due to the splitting ΔM being close to the pion mass. This coincidence, while eliminating the final state particles as a detection path, leaves another possibility open. Because of the constrained phase space available for the decay products, the lifetime of the charged state is relatively long. Therefore, searches for such particles could look for a charged particle traveling through the central tracker and then disappearing – a stub in the tracker. With two charged final state particles there would of course be two stubs.

Such searches will of course be challenging. While a $c\tau$ of 10 cm is huge compared to the lifetimes of SM particles, it is small compared to the physical size of the detector. The ATLAS central tracker consists of three silicon pixel layers in the barrel at a distance of 5.05, 8.85, and 12.25 cm from the beam, followed by four layers of the silicon central tracker (SCT) at 29.1, 37.1, 44.3, and 51.4 cm [26]. Thus, most of the X_3^+ decays would occur before the SCT, and only $\sim e^{-5}$ of all particles would reach the Transition Radiation Tracker (TRT) at 56.3 cm. Despite the great differences in design in the outer sections (most significantly in the muon systems), the CMS detector is similarly configured in the central tracking region, with three pixel layers at 4.4, 7.3, and 10.2 cm, while the first layer of the silicon strip tracker is at 22 cm [25]. As the two central tracking regions are so similar, we use the slightly more conservative (for our purposes) ATLAS distances.

Since the only visible signature of X^+X^- production is stubs, production of these particles would be missed given current triggers. In order to record production events, we therefore require at least one associated jet produced by initial state radiation, *i.e.* $pp \to X_3^+ X_3^- +$ jets. The idea would be to trigger on jet energy or missing energy, but identify the stubs off-line to distinguish signal events from the abundant jet or missing energy background.

As production proceeds via weak couplings, the additional requirement of associated jets greatly reduces an already small cross section (especially for the larger values of M). We therefore consider only unprescaled triggers. We choose a missing transverse energy (MET) trigger, requiring MET$>$ 65 GeV in the high luminosity mode [27]. We select MET rather than jet p_T because of the lower (net) jet energy specified to pass the trigger cut.

Nonetheless, this trigger may turn out to be overly aggressive, so the scaling of production cross section with a variety of trigger options for $M = 300$ GeV is shown in Table I. Also in Table I, we give the cross sections for center of mass energies of 10 TeV and 13 TeV, for the various trigger selections.

$\sqrt{s}$ (TeV)	MET$>$ 65 GeV	MET$>$ 80 GeV	Jet $p_T > 110$ GeV	jet $p_T > 150$ GeV
13	50.2 fb	44.1 fb	34.2 fb	23.9 fb
10	26.5 fb	23.1 fb	17.1 fb	11.5 fb

TABLE I: The production cross section of $X_3\bar{X}_3$ pairs at $\sqrt{s} = 13$ TeV and 10 TeV with $M = 300$ GeV using four different trigger menus. These are triggers on MET$>$ 65 GeV, MET$>$ 80 GeV, highest jet $p_T > 110$ GeV, and a highest jet $p_T > 150$ GeV. All cross sections were calculated using MadGraph [28] and Pythia [29]. See text for further details.

We see that we expect a reasonable number of such events for particle masses of order a few hundred GeV. We now consider the cross sections with the restrictions on the stubs necessary to detect the signal events.

The principal requirement is that both tracks must pass through at least three layers of the central tracker so that the stubs are sufficiently long to be found in an off-line analysis. This requires the transverse physical track lengths ($\beta\gamma c\tau \sin\theta$, where θ is the polar angle measured from the beam line) to be greater than 12 cm. In the remainder of this paper, we will refer to this quantity as transverse $c\tau$, or $Tc\tau$. One should bear in mind that conventional track reconstruction algorithms require hits in all the central tracker layers. Without a detailed detector simulation or data analysis it is difficult to know with certainty that three hits will be sufficient to identify signal events and distinguish them from background, but in the interest of maximizing signal we first explore this possibility.

However, experimental groups might find more hits necessary for purposes of background rejection, track reconstruction, and charge assignment (as longer tracks provide a better handle on the track curvature, and thus sign of the charge). The next layer (the fourth from the center and the first of the SCT) lies at 30 cm at ATLAS. Due to the slightly more compact design, this transverse distance would cross two additional tracker layers at CMS, for a total of five hits. In both cases we expect a serious decrease in the cross section of events with 4 hits on both tracks. We will show the expected cross section requiring $Tc\tau > 30$ cm on both tracks, as well as events with one stub of 12 cm and 30 cm on the other. Thus, in addition to the $\min[Tc\tau] > 12$ cm cut, we also show results for $\min[Tc\tau] > 30$ cm and $\{\min[Tc\tau] > 12 \text{ cm}, \max[Tc\tau] > 30 \text{ cm}\}$.

In all cases, we require both tracks to have $|\eta| < 2.5$ so that they sit in the central barrel, where the tracking layers are closest to the interaction point. Our final requirement is that $\Delta R > 0.4$, where ΔR is the minimum $\phi - \eta$ angular distance between both tracks and any jet, so that the two tracks are isolated from all jets in the event.

In Figure 3, we plot the differential cross section for X^+X^- + jets production as a function of $Tc\tau$ for each event for $M = 200, 300, \ldots, 1000$ GeV to give an idea of the distribution of path lengths. In Figure 4, for the same range

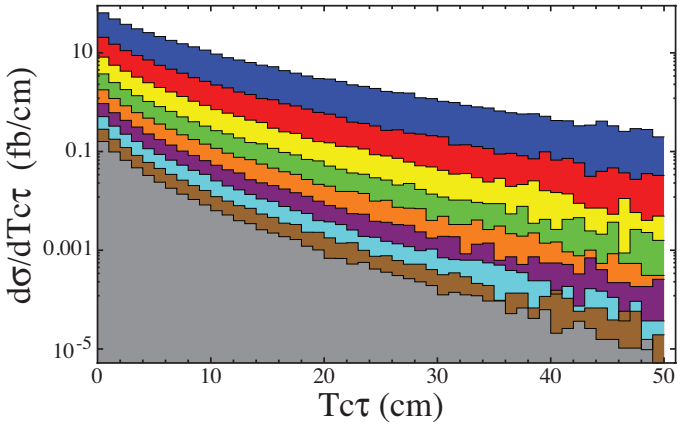

FIG. 3: Differential cross section versus transverse path length $Tc\tau$ of $X_3^{\pm}$ from $X_3^+X_3^-$ +jets events at $\sqrt{s} = 13$ TeV, triggering on 65 GeV MET signature. Cuts of $\Delta R > 0.4$ and $|\eta| < 2.5$ have been applied, but no cut on $Tc\tau$ has been added (see text for more detail). Color coding denotes mass of X_3^0 state: blue is 200 GeV, red is 300 GeV, yellow 400 GeV, green 500 GeV, orange 600 GeV, purple 700 GeV, cyan 800 GeV, brown 900 GeV, and grey 1000 GeV.

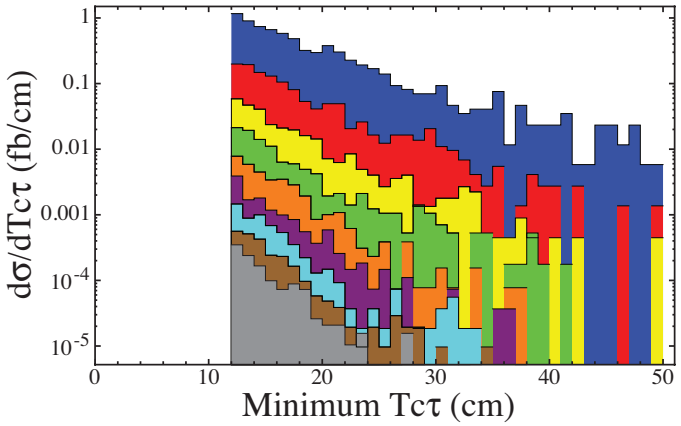

FIG. 4: Differential cross section versus the minimum value of $Tc\tau$ of $X_3^+X_3^-$ pairs. $X_3^+X_3^-$ + jets events were generated at $\sqrt{s} = 13$ TeV, with 65 GeV MET triggering. Cuts on $\Delta R > 0.4$, $|\eta| < 2.5$, and $\min[Tc\tau] > 12$ cm have been applied. Color coding for X_3 mass as in Fig. 3.

of masses, we plot the differential cross section as a function of minimum $Tc\tau$ of each $X_3^+X_3^-$ pair for those events passing the cuts above.

In Table II, we give the integrated cross sections for the events passing our cuts as a function of mass. We provide integrated cross sections for the $\min[Tc\tau] > 12$ cm, $\min[Tc\tau] > 30$ cm, and $\{\min[Tc\tau] > 12$ cm, $\max[Tc\tau] > 30$ cm$\}$ cuts. Extrapolating these results, and assuming that five of these isolated, opposite sign, three-hit tracks are sufficient for discovery, an integrated luminosity of 10 fb^{-1} is sufficient to discover X_3 triplets with a mass of ~ 350 GeV at the LHC, With 100 fb^{-1} triplets with masses up to 550 GeV are in reach. Requiring two tracks with four hits each ($\min[Tc\tau] > 30$ cm) reduces our reach to 200 GeV for 10 fb^{-1} and 300 GeV for 100 fb^{-1}. In both cases, these results constitute significant advances on the current exclusion regions.

Figure 4 and Table II are the main results of this section. At this point, we go into more detail on the techniques used to simulate the production of the $X_3^+X_3^-$. Using our own model files, $X_3^+X_3^-/X_3^{\pm}X_3^0$ + jets Feynman diagrams were generated using MadGraph [28]. At the partonic level, we restricted ourselves to one or two jets (inclusive), due to computing constraints on generating events with higher jet multiplicity.

For each choice of X_3^0 mass (*i.e.* 200, 300, ..., 1000 GeV), the mass splitting (and thus the mass of the $X_3^{\pm}$) and decay width were calculated using Eqs. (4) and (6). For each mass, 100,000 events were generated in MadGraph, requiring partonic jet $p_T > 15$ GeV, $|\eta| < 5$, and $H_T > 50$ GeV (here H_T is defined as the magnitude of the vector sum of all jet p_T). The large event sample was necessary in order to gain meaningful statistics after the severe cuts.

The underlying event and jet showering were provided by running the MadGraph samples through stand-alone Pythia 6.409 [29]. Jet-finding was through Pythia's built in cell algorithm, with an R value of 0.4. The p_T cut-off for

X_3^0 Mass (GeV)	σ_{12} (fb)	σ_{30} (fb)	$\sigma_{12/30}$ (fb)
200	8.8	0.69	4.0
300	1.4	0.062	0.45
400	0.32	0.013	0.10
500	0.11	0.0037	0.029
600	0.036	0.0005	0.0062
700	0.013	0.0001	0.0025
800	0.0059	0.0000	0.0010
900	0.0025	0.0000	0.0005
1000	0.0012	0.0000	0.0002

TABLE II: The integrated cross sections for $X_3^+X_3^-$ +jets events in which min$[Tc\tau] > 12$ cm (σ_{12}), as well as min$[Tc\tau] > 30$ cm (σ_{30}); and min$[Tc\tau] > 12$ cm, max$[Tc\tau] > 30$ cm ($\sigma_{12/30}$), as a function of mass. Events were simulated at $\sqrt{s} = 13$ TeV with a MET trigger of 65 GeV. In addition to the $Tc\tau$ requirement, events passed an $|\eta| < 2.5$ cut on $X_3^\pm$ and an isolation cut of $\Delta R > 0.4$. The corresponding differential cross sections are shown in Fig. 4.

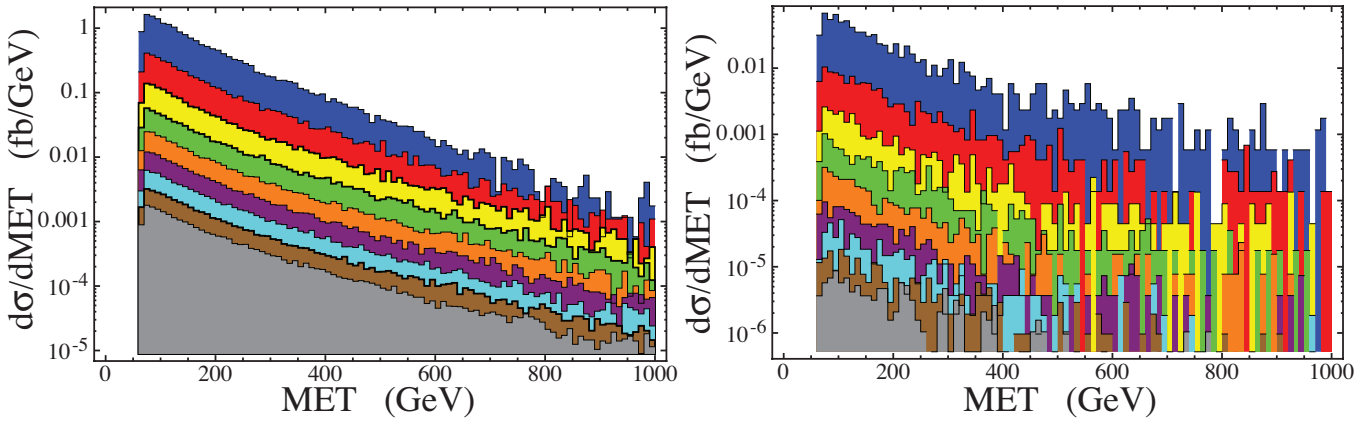

FIG. 5: Left: Missing transverse momentum (MET) of $X_3^+X_3^-$ + jets events passing MET> 65 GeV trigger as well as $X^\pm$ $|\eta|$ and isolation cut at $\sqrt{s} = 13$ TeV. Right: MET distribution of those same events after application of a cut requiring both X_3^+ and X_3^- have $Tc\tau > 12$ cm. Color coding denotes choice of X_3^0 mass and is the same as in Fig. 3.

generation of the underlying event was set at 15 GeV. Decay of the charged triplets was done through the standard Pythia decay routines, with the width and lifetime set by hand. MadGraph's integrated Pythia and PGS options were not appropriate in this case, as PGS in particular does not have the correct response to new stable particles which reach the detector.

For all cuts based on jet p_T, the relevant values were taken from the Pythia-identified jets, not from the parton-level. The value of missing transverse energy for trigger purposes was obtained for each event by taking the magnitude of the vector sum of jet p_T for all jets with $|\eta| < 5$ and $p_T > 20$ GeV. After determining whether an event passed the trigger, subsequent cuts on $X_3^\pm$ isolation and $|\eta|$ were applied. Finally, a cut on the minimum $Tc\tau$ of both charged triplets in $X_3^+X_3^-$ events was performed. As outlined previously, the benchmark requirement of both particles passing three layers corresponds to the minimum transverse $c\tau$ being greater than 12 cm, while at ATLAS four hits on both tracks corresponds to 30 cm. A third option is to apply a cut requiring one track to be longer than 12 cm, and the other longer than 30. For our benchmark trigger, we use require MET> 65 GeV. For other trigger options, see Table I. The differential distributions of MET before and after the $Tc\tau$ cut are displayed in Fig. 5.

In Fig. 6, the jet p_T and $|\eta|$ differential distributions for events both before and after the min$[Tc\tau] > 12$ cm cut are shown. Fig. 7 shows the differential distribution of the minimum value of p_T and maximum value of $|\eta|$ for the $X_3^+X_3^-$ pair, again before and after the application of the $Tc\tau$ cut. The effect of the $Tc\tau$ cut is (besides reducing the overall number of events) to push the η distribution to lower values and the p_T distribution upward. This is as expected, as the $Tc\tau$ constraint can more easily be satisfied by $X_3^\pm$ traveling in the central region. The histogram bins have been weighted by total cross section and total number of generated events for each mass choice. Note that small statistics become an issue after all cuts are applied.

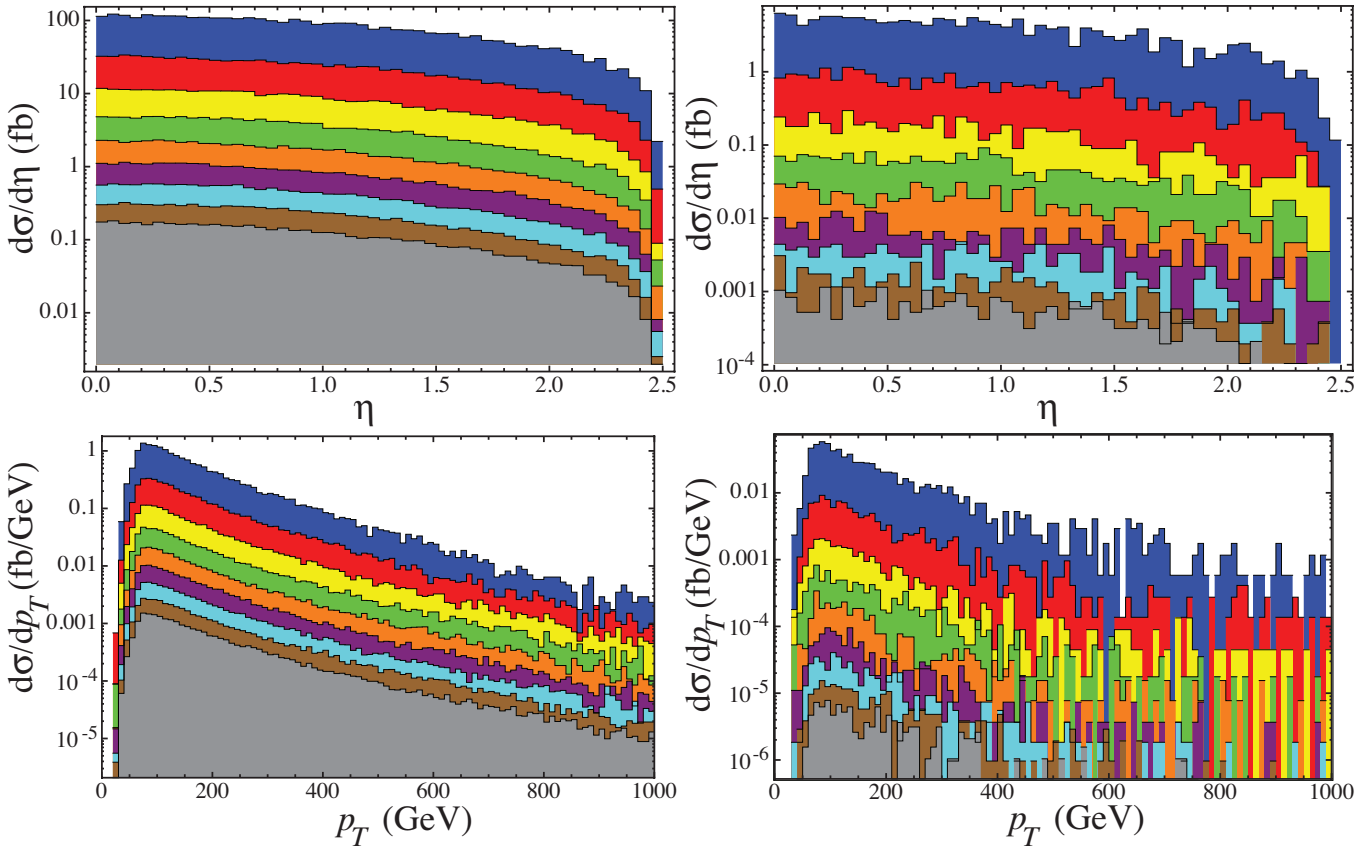

FIG. 6: Upper left: $|\eta|$ of highest p_T jet for $X_3^+ X_3^-$ +jets events passing MET> 65 GeV trigger as well as $X^\pm$ $|\eta|$ and isolation cut at $\sqrt{s} = 13$ TeV. Lower left: p_T of highest p_T jet from these events. Upper right: $|\eta|$ of highest p_T jet from events that pass all cuts applied previous, plus the requirement that $Tc\tau > 12$ cm for both X_3^+ and X_3^-. Lower right: p_T of highest p_T jet from those same events. Color coding denotes choice of X_3^0 mass and is the same as in Fig. 3.

It is difficult to determine the background rate for these stub events. From a purely theoretical standpoint, there are no irreducible backgrounds, as no SM particles have $c\tau$ lengths that can compete with that of the triplets. However, there might be a large background of low energy charged particles from the underlying event, which will cause random hits in the inner detector layers. These random hits could coincidentally line up in the pixel tracker and register a fake event.

The number of such fake tracks will likely remain unknown without experimental measurement of the characteristics of the underlying event. However, by exploiting the random nature of the background events, the tracks resulting from the true triplets may be distinguished. We propose a few possible techniques here.

The random nature of the fakes means that, even if two such false tracks appear in a single event, it is highly unlikely that they will correctly point back to the primary vertex (identified as the origin of the trigger jets). High p_T tracks, such as the ones we are interested in, do not bend much inside the magnetic field of the detector. While this makes the measurement of p_T difficult, it does mean that the track vertex can be identified to within 50μm [30]. Since much of the background noise in the event will presumably be due to pile-up, with up to 12 interactions separated by 5 mm on average, this ability to unambiguously identify the primary vertex should allow some subtraction of activity due to multiple interactions.

By requiring two stubs in each event, the number of fake events passing our cuts can be reduced. If charge information for each track can be obtained we would have an additional handle to identify background, as the true triplet events must have one positive and one negative particle. This may be aided by the requirement of 4-hit or 5-hit tracks, since charge will be measured by the curvature of the particle as it moves through the detector. With only three hits, charge determination may be difficult or impossible. As mentioned, long tracks come at a significant price in event rate. Also, we found no study on the effectiveness of charge discrimination on massive particles using only the inner tracking layers, making the efficiency of this technique unknown.

Once we have a possible signal in the two-stub channel, we can gain confidence that it is in fact new physics by considering the single-stub events. In our simple models we can make precise predictions of how many single track

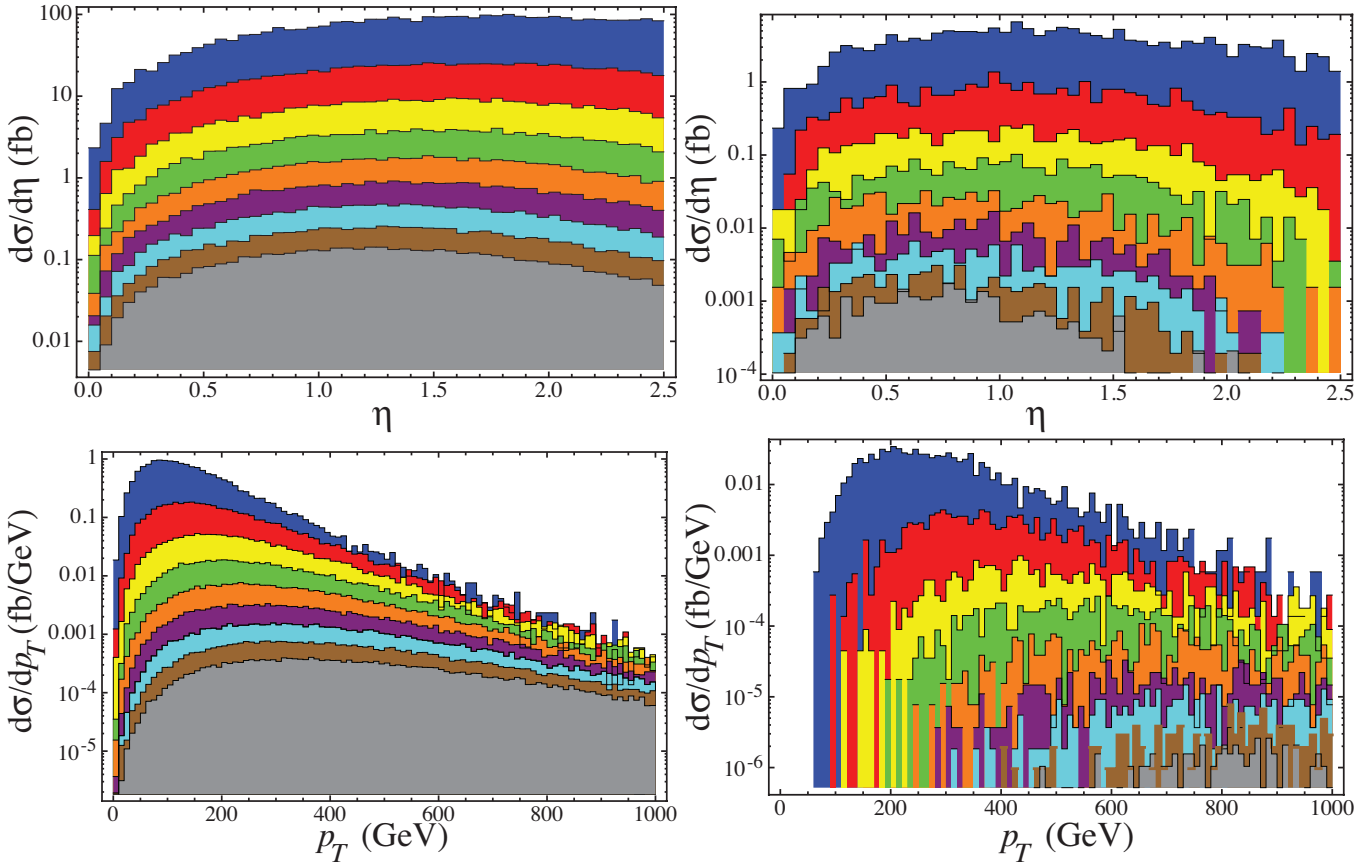

FIG. 7: Upper left: Maximum $|\eta|$ of $X_3^\pm$ from $X_3^+X_3^-$ + jets events passing MET> 65 GeV trigger as well as $X^\pm$ $|\eta|$ and isolation cut at $\sqrt{s} = 13$ TeV. Lower left: Minimum p_T of $X_3^\pm$from these events. Upper right: Minimum $|\eta|$ of $X_3^\pm$ from events that pass all cuts applied previous, plus the requirement that $Tc\tau > 12$ cm for both X_3^+ and X_3^-. Lower right: Minimum p_T of $X_3^\pm$ from those same events. Color coding denotes choice of X_3^0 mass and is the same as in Fig. 3.

events with $Tc\tau > 12$ cm should be present compared to double-tracks. Naively, the ratio should be about $4:1$ (X^+X^0, X^-X^0, and X^+X^- where one particle decays quickly). In reality, the ratio is skewed: among other reasons, the X^+X^0 events are produced more copiously than X^-X^0, as the LHC is a $p-p$ machine, not $p-\bar{p}$. From simulation, we find approximately 5.5 single track events for every double track event in the triplet scenario. Additional subtleties would arise if the new physics is some higher multiplet of $SU(2)_L$, with several possible charged states. Observation of a pattern would give us more reason to believe that the signal is in fact a sign of new physics, rather than arising from background.

Additional confidence in our signal might be obtained by comparing the number of single tracks passing through four and five layers with the number passing through three. Since this distribution should follow an exponential decay curve, it may be possible to confirm that the signal seen in the pixel detector is in fact not background.

These techniques, which all rely on the random nature of the spurious track background, may provide tools which will determine whether a sample of short tracks originates from new physics of the type exemplified by the triplets. However, as stated previously, the true background to the $X_3^+X_3^-$ tracks cannot be reliably estimated without actual experimental data. Moreover the exponential tail will have large fluctuations for small event numbers. Thus, all these methods for background reduction are necessarily somewhat speculative and we hope there will be a more rigorous study by the two experimental collaborations.

We now turn to the discovery potential of the X_2 doublets. Recall the doublets have larger mass splitting and are thus more difficult to detect. Nonetheless, the current bounds are so weak that we can still place an interesting bound light doublets. At low enough mass, the LHC will have a large enough production cross section so that a sufficient number of double pairs on the exponential tail will make it through all three layers.

The key requirement of the triplet discovery was the $\min[Tc\tau] > 12$ cm for $X_3^\pm$.[2] A quick comparison of the decay length of the doublets $X_2^\pm$ with that of the triplets (as seen in Fig. 2) makes it clear that such a strategy will be less promising for doublet searches. The difference in $c\tau$ can be traced to the non-zero hypercharge of X_2, which leads to a larger mass splitting (Eq. (4)).

In Fig. 8, the total differential cross section for $X_2^\pm$ as a function of $Tc\tau$ is shown. As the characteristic distance traveled is on the order of 1 cm, the cross section for events where both X_2^+ and X_2^- survive a $Tc\tau$ distance of 12 cm is suppressed by a factor of approximately $e^{-2\times 12/1}$ compared the production cross section. With this suppression (compared to that of $e^{-2\times 12/10}$ for the triplet case), almost no doublet events survive the application of the $Tc\tau$ cuts. For the smallest choice of mass we explored in the triplet case, $M = 200$ GeV, we find only four events out of the 100,000 generated that passed all cuts, giving a nominal cross section of ~ 0.02 fb for events with $\min[Tc\tau] > 12$ cm.

We therefore restrict our attention to a lower mass, 100 GeV. This permits sufficient events to be seen for two reasons. First, the characteristic $c\tau$ increases with lower mass (see Fig. 2), from ~ 1 cm when $M = 200$ GeV to 1.8 cm when the mass is 100 GeV. Second, lower mass particles have a much larger production cross section, increasing the probability that some events will contain an $X_2^+X_2^-$ pair that both survive long enough to hit the requisite three layers. After applying the now-standard cuts on η, ΔR, and $\min[Tc\tau] > 12$ cm, we find a total cross section of 0.4 fb. At CMS, the third layer of the pixel is slightly closer to the beam, at 10 cm, rather than 12. While this has a negligible effect for long life-time triplets, it amounts to approximately one lifetime for the doublets. Using the CMS distance, we require $\min[Tc\tau] > 10$ cm and find a cross section of 0.9 fb. From this we conclude that the LHC will be able to probe doublet models up to about ~ 100 GeV. While this is much worse than the reach of triplet models, it nonetheless improves on the current bound of 70 GeV which can be obtained from LEP-II [22].

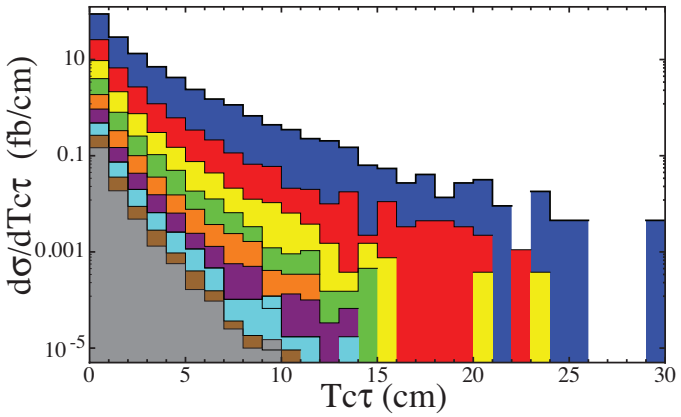

FIG. 8: Differential cross section versus transverse path length $Tc\tau$ for $X_2^\pm$ from $X_2^+X_2^-$ +jets events at $\sqrt{s} = 13$ TeV, triggering on 65 GeV MET signature. Cuts of $\Delta R > 0.4$ and $|\eta| < 2.5$ have been applied, but no cut on $Tc\tau$ has been added (see text for more detail). Color coding is as in Fig. 3.

The discovery potential is effectively set by the value of ΔM (via its effect on the width and thus decay distance $Tc\tau$). This accounts for the large difference in experimental sensitivity between triplets and doublets. In the next section we consider relaxing the constraint between M and ΔM. This allows us to explore interpolating cases between the ~ 150 MeV splitting of triplets to the ~ 300 MeV splittings of doublets, and investigate the range of mass splittings which the LHC can probe, as well as consider the possibility of an anomaly-mediated wino LSP scenario.

IV. PERTURBATIONS ON A THEME

If we assume that lepton number is an exact symmetry (or alternatively, that the X fields have their own global symmetry that translates to a conserved quantum number), no tree-level terms can be added to Eq. (1). Higher-dimensional terms such as $HHX\bar{X}$ (where H is the SM Higgs) are possible, but do not cause an additional splitting between the neutral and charged components.

[2] Tracks passing four or more layers are exponentially suppressed and have essentially zero cross section for the doublet models. We shall therefore only consider the three-layer tracks from this point on.

However, a tree-level contribution to the splitting is possible when there is more than one new $SU(2)_L$ multiplet. Consider the case when both X_2 and X_3 are present in the spectrum; with tree-level masses M_2 and M_3 respectively. Then the Lagrangian becomes

$$\mathcal{L} = i\bar{X}_2 \not{D} X_2 + i\bar{X}_2 \not{D} X_3 - M_2 \bar{X}_2 X_2 - M_3 \bar{X}_3 X_3 + yH\bar{X}_2 X_3 + \text{h.c.} \tag{10}$$

Once the Higgs field obtains its vacuum expectation value v, the charged and neutral doublets and triplets mix. Assuming the combination yv is small compared to M_2 or M_3, the splitting between the lowest charged and neutral eigenvalues is yv.

This effect can be realized in supersymmetry, which has vector fermions in the form of the triplet winos $\tilde{W}$ and the doublet higgsinos $\tilde{H}_u$ and $\tilde{H}_d$ (the presence of two doublets is only a minor complication). As we are interested in the phenomenology of a charged particle decaying into a stable neutral state, we only explore when the LSP $\tilde{\chi}_1^0$ and NLSP $\tilde{\chi}_1^\pm$ are linear combinations of $\tilde{W}^0/\tilde{H}^0$ and $\tilde{W}^\pm/\tilde{H}^\pm$ respectively. This can be arranged by setting the gaugino mass $M_2 < |M_1|, |\mu|$ (we also assume M_2 is real and positive). For simplicity, we assume that all other supersymmetric masses are large.

As a specific example,[3] a wino LSP can be realized in anomaly-mediated supersymmetry [18, 19], where the gaugino masses M_i are

$$M_i = -b_i g_i^2 M_{\text{SUSY}}. \tag{11}$$

Here M_{SUSY} is the overall SUSY breaking scale, $i = 1, 2, 3$ are the $U(1)_Y$, $SU(2)_L$, and $SU(3)_C$ gauge groups (with couplings g_i) respectively, and b_i are the one-loop β function coefficients. This leads to a mass ratio of $M_1 : M_2 : M_3 = 3.3 : 1 : -10$.

The tree-level mass matrix for the neutralinos in the $(-i\tilde{B}, -i\tilde{W}^3, \tilde{H}_1^0, \tilde{H}_2^0)$ is

$$\mathbf{M}_{\tilde{\chi}^0} = \begin{pmatrix} M_1 & 0 & -m_Z c_\beta s_W & m_Z s_\beta s_W \\ 0 & M_2 & m_Z c_\beta c_W & -m_Z s_\beta c_W \\ -m_Z c_\beta s_W & m_Z c_\beta c_W & 0 & -\mu \\ m_Z s_\beta s_W & -m_Z s_\beta c_W & -\mu & 0 \end{pmatrix} \tag{12}$$

where $c_\beta = \cos\beta$, $s_\beta = \sin\beta$, $c_W = \cos\theta_W$ and $s_W = \sin\theta_W$. The mass matrix for the charginos in the $(-i\tilde{W}^\pm, \tilde{H}^\pm)$ basis is

$$\mathbf{M}_{\tilde{\chi}^\pm} = \begin{pmatrix} M_2 & \sqrt{2} m_W s_\beta \\ \sqrt{2} m_W c_\beta & \mu \end{pmatrix}. \tag{13}$$

Clearly, we could diagonalize $\mathbf{M}_{\tilde{\chi}^\pm}$ and $\mathbf{M}_{\tilde{\chi}^0}$ to find the mass difference $\Delta M_{\text{tree}} \equiv m_{\tilde{\chi}_1^\pm} - m_{\tilde{\chi}_1^0}$. In the limit of large $|\mu|$, a useful analytic expression can be obtained by expanding the mass difference in terms of inverse powers of μ. We find that the μ^{-1} term vanishes, and the first non-zero term is

$$\Delta M_{\text{tree}} = \left(M_2(1 - \sin 2\beta) + \frac{m_W^2 \tan^2\theta_W}{(M_1 - M_2)} \sin^2 2\beta \right) \frac{m_W^2}{\mu^2}. \tag{14}$$

This is in addition to the loop splitting of Eq. (4). We see that, if M_1 and M_2 are $\mathcal{O}(100\text{ GeV})$ while $|\mu|$ is $\mathcal{O}(\text{TeV})$, then ΔM_{tree} is of the same order as the loop contribution: a few hundred MeV.

By appropriate choices of the magnitudes and signs of M_1, M_2, μ, and $\tan\beta$ (perhaps requiring us to relax the anomaly-mediated predictions for the relative size of M_1 and M_2) we can effectively dial the total mass splitting. This sets the scale of $Tc\tau$ and, as seen in Section III, controls whether a particular model can be discovered at the LHC.

If we strictly abide by the gaugino mass ratio of $3.3 : 1 : -10$ in anomaly mediated supersymmetry breaking, then from Eq. (14), we see that the tree level splitting can only be positive. Added to the triplet loop-induced splitting, this means that the pion channel is always open to the NLSP. In order to close this channel, the tree contribution would have to be negative, requiring $M_2 > M_1$, which does not occur in a conventional anomaly-mediated spectrum.

To explore the dependence of an LHC discovery on ΔM, we consider SUSY spectra with a fixed mass of the neutralino LSP $\tilde{\chi}_1^0$ and vary the mass of the NLSP $\tilde{\chi}_1^\pm$. To discuss experimental reach, we first treat ΔM as a free parameter. Afterwards we will consider what ranges of anomaly-mediated input parameters that the LHC can access.

---

[3] This derivation follows that of [13].

The full spectrum was calculated using SuSpect 2.41[31], with input parameters tuned to give the required splittings. As we are taking our cue from anomaly mediated scenarios with the hierarchy $|M_2| < |M_1| \ll |\mu|$, the sfermions tend to be very massive ($\gtrsim$ 2 TeV). This is not always true, for the lightest neutralinos with masses near the current experimental bounds ($\sim$ 100 GeV [20]) the squark masses in an anomaly mediated spectrum must be on the order of 500 GeV for $\Delta M \sim 200$ MeV, and 1500 GeV for splittings of 350 MeV. However, in all cases we investigated, the sfermions decouple from the low energy theory and do not greatly affect the production cross section. Even in the previous examples, changing the lightest squark mass from 500 GeV to 1500 GeV while keeping the LSP/NLSP masses at 100 GeV increases the total production cross section by only 2%.

We set the LSP mass $m_{\tilde{\chi}_1^0}$ equal to 100, 200, 300, and 400 GeV. In all cases, we generate 100,000 $\tilde{\chi}_1^+\tilde{\chi}_1^-$ + jets events in MadGraph at $\sqrt{s} = 13$ TeV. After event generation, we vary the mass splitting ΔM from 145 to 220 MeV. Such change has no appreciable effect on the kinematics of an individual event with the exceptions of the energy of the light decay products and the decay length. The latter, of course, is the parameter of interest in our study while the former can be ignored, as the pions cannot be used in track identification. The key point here is that, if ΔM is the only parameter that is adjusted, any event that passed the acceptance cuts (*i.e.* MET trigger, ΔR, $|\eta|$) will continue to do so; changing ΔM affects only whether a particular event will pass the $Tc\tau$ cuts.

After selecting a mass difference, we then apply a MET> 65 GeV trigger, as well as the η, jet isolation, and $Tc\tau$ cuts as outlined in Section III. The resulting cross sections of events with two charged tracks with min$[Tc\tau] > 12$ cm are displayed in Fig. 9.

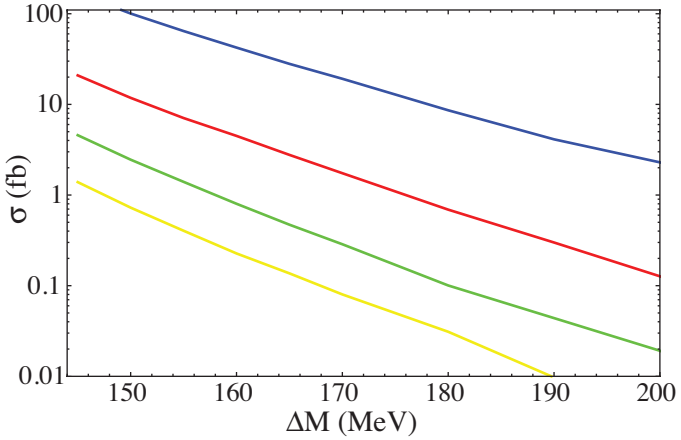

FIG. 9: Cross section of $\tilde{\chi}_1^+\tilde{\chi}_1^-$ + jets passing MET> 65 GeV trigger as well as $|\eta|$ and isolation cut at $\sqrt{s} = 13$ TeV as a function of mass splitting $\Delta M \equiv m_{\tilde{\chi}_\pm^0} - m_{\tilde{\chi}_1^0}$. The blue lines corresponds to a neutralino mass $m_{\tilde{\chi}_1^0} = 100$ GeV, while red is 200 GeV, green 300 GeV, and yellow 400 GeV.

Assuming 10(100) fb^{-1} of luminosity, we find that a 400 GeV NLSP can be discovered only if the splitting is less than $\sim$ 155(175) MeV (again, assuming 5 events are required). A 100 GeV NLSP can be discovered if the splitting is larger, on the order of 220 MeV for the lower luminosity, and perhaps as high as 240 MeV for 100 fb^{-1}. Due to the exponential fall off on the numbers of events as we go to larger splittings, small statistics become an issue.

From these results, we can also determine the range of anomaly-mediation parameters that the LHC should probe. The loop-induced mass splitting for a 100 GeV triplet is 145 MeV, meaning that the LHC will be sensitive to a tree-level splitting of 75 MeV. From the splitting between the lightest eigenvalues of the neutralino and chargino mass matrices (Eqs. (12) and (13)), we see this splitting corresponds to $|\mu| \gtrsim 5$ TeV for $\tan\beta = 10$. For a 400 GeV neutralino, the LHC would be sensitive a tree-level splitting less than 15 MeV (at high luminosity), which requires $|\mu| \gtrsim 6$ TeV.

Assuming a universal scalar mass m_0, then the wino mass M_2 can be related (via the anomaly mediation mass $M_{\rm aux}$) to the μ parameter and m_0 by the requirements of EWSB. For $m_0 \lesssim 2$ TeV and wino masses of $\mathcal{O}(100$ GeV), the required $|\mu|$ value tends to be much less than the $5-6$ TeV required for sufficiently small ΔM. As a specific example, for sgn$(\mu) < 0$ (preferred from $b \to s\gamma$ for large $\tan\beta$), $\tan\beta \gtrsim 10$, $m_0 < 2$ TeV, and a wino mass of 400 GeV corresponds to $\mu \sim -2500$ GeV [32]. At the lower end of the wino mass scale, $M_2 = 100$ GeV corresponds to $\mu \sim -600$ GeV for the same parameters.

When m_0 is relatively small leading to a more natural spectrum, the stub signature for anomaly mediated degenerate winos is between a rock and a hard place. If $|\mu|$ is small enough to allow for a light NLSP (and thus a large cross section at the LHC), the splitting will be large, and the NLSP will decay rapidly and invisibly to the LSP. On the

other hand, if the μ parameter is large, the chargino's $c\tau$ will be big, but the overall rate of production will be too small for meaningful statistics to be collected.

In order to have $|\mu| \sim 5$ TeV (and thus the requisite small ΔM), with the wino spectrum sufficiently light to be visible [m_0 would need to also be around 5 TeV. This would create an unnatural spectrum, with heavy scalars of $\mathcal{O}(5$ TeV) and light gaugino masses of a few hundred GeV.

One can have satisfactory and visible anomaly-mediated-based models when they are supplemented by a non-universal scalar mass. Relaxing the requirement of universal m_0 masses would allow the squarks and sleptons to remain light although the Higgs mass would still be unnaturally big.

If we abandon anomaly-mediation altogether, then we are no longer bound by the relation between M and ΔM shown in Eq. (14), and we may take our results for maximum ΔM as a function of M as the expected reach of the LHC for degenerate chargino/neutralino pairs. Implicit in this statement is the assumption that the squarks and sleptons are much more massive than the winos. If they are not then the overall production cross sections must be adjusted accordingly.

Additionally, if M_2 is no longer required to be larger than M_1, there is the possibility that the tree level splitting is negative. In this case, in addition to the splittings investigated above (which are all larger than the loop-level contribution), we have the possibility of splittings smaller than the pion mass. In such cases, detection would be straightforward. With $\Delta M < m_\pi$, and the decay proceeds through the $\tilde{\chi}_1^0 \ell \nu_\ell$ three-body final state. From Fig. 2, we see that the charginos will travel on the order of several meters before decaying. Stubs would no longer be the signal for this model.

To demonstrate this possibility, we consider an LSP mass of 400 GeV and $\Delta M = 100$ MeV. With a MET$>$ 65 GeV cut, the production cross section for $\tilde{\chi}_1^+ \tilde{\chi}_1^- +$ jets events passing the $|\eta|$ and isolation cuts is 10.0 fb. Of these events, 8.1 fb have both $\tilde{\chi}_1^\pm$ states decay after the requisite 12 cm $Tc\tau$ cut, and 0.04 fb after 10 meters (the characteristic distance to the muon system at ATLAS). The total cross section for metastable charged particles at the LHC will in fact be larger, since it will be possible to trigger on the heavy particles themselves, rather than the associated jet production. These events would show up in the muon system as heavy, slow 'muons,' essentially identical to the expected signature of new stable charged particles. The current lower bound on the mass of wino-like stable LSP/NLSP pairs is 206 GeV from D0 [33], expected to rise to ~ 600 GeV at the LHC (at $\sqrt{s} = 14$ TeV) [34]. As the searches for stable charged particles differ significantly from the stub searches required for unstable particles, we do not consider this scenario further here. However, we do note that the presence and $Tc\tau$ distribution of charged tracks which disappear in flight may provide a method of determining the lifetime and mass splittings if the 'stable' charged particles are in fact merely a long-lived (on detector timescales) NLSP.

V. CONCLUSIONS

New weakly charged multiplets with nearly degenerate masses are an excellent example of non-standard new physics at the TeV-scale that might be produced at the LHC yet evade observation with current search strategies. Though not required by most solutions to the hierarchy, naturalness, and dark matter problems, they might exist and could be within observable reach. Search strategies for such particles certainly merit consideration.

In the simple models considered in this paper, *i.e.* the minimal examples with $SU(2)_L$ doublets or triplets, the new multiplets do not have any strongly-coupled production mechanism. Furthermore, their small mass splittings lead to very low energy SM decay products in addition to the invisible neutral state. While the anomaly-mediated models do contain strongly coupled states (gluinos and squarks), these particles could be too heavy to be produced in large numbers at the LHC.

Discovery of these models through standard techniques is impossible. The weak production cross section means that the contribution to jets+$\not{E}_T$ would be swamped by SM processes, and the low energy decay products are completely lost in the noisy underlying event. Note that larger representations of $SU(2)_L$ face the same issues. Without much higher luminosity or energy, we don't expect even representations to be visible since their width (for a given mass) should be at least as large as in the doublet case. For odd multiplets with zero hypercharge, the mass difference between the lowest charged and neutral states is the same as for the triplet, but both production and decay widths will be bigger (due to the larger Casimir) so the searches will not be manifestly simpler, and in fact may have more in common with the doublet searches than the triplets.

In this paper we discussed a potentially promising approach for discovering vector multiplets at the LHC with nearly degenerate elements that focuses on the short charged tracks formed by the charged component. Though standard track-reconstruction techniques require hits in all layers of the inner detector which correlate with energy deposition in the calorimeters or activity in the muon chamber, it should be possible to relax these constraints. We suggest that the nearly degenerate particles could be found by the ATLAS and CMS collaborations using the high resolution of the inner pixel detector in order to find 'stub' tracks passing through the first three detector layers, using a missing

E_T trigger to write the event to tape. With off-line analysis, one should be able to identify events containing two isolated, charged high p_T stubs.

Background rejection will be a major issue, and the rate of fake events is difficult to estimate without experimental data. We expect that the probability of two short tracks being formed by random hits is very small, but at the present, this is mere conjecture. Whatever the rate, requiring that the tracks and jets share a common primary vertex should help reduce background. Requiring unlike charges on the tracks would also help, though this measurement is expected to be very difficult due to the stiffness of the high p_T particles. If necessary, stubs passing through four or more layers could be used, although this will come at a significant sacrifice of event rate.

Because of the dependence of particle lifetime on mass splitting in the multiplet, the requirement that the charged particle pass at least three layers of the pixel tracker makes the mass splitting ΔM the linchpin of the discovery potential. For $\Delta M \sim 150$ MeV, as in the case of triplets, the new multiplets can be seen for masses below 350(550) GeV with 10(100) fb^{-1} of data. This reach drops precipitously with increasing ΔM; $SU(2)_L$ doublets have splittings on the order of 300 MeV, and for masses much greater than 100 GeV they are invisible at the LHC. Larger splittings are likewise undetectable, until multi-particle modes open at around ~ 1 GeV. However, the background for particles that decay into low energy multi-hadron states with large impact parameters is unknown, and we have not considered such searches in this paper. Of course, for $\Delta M < m_\pi$, the lifetime is long enough to pass through all of the central tracker and even into the calorimeters and muon system. Discovery is then relatively straightforward, subject to the same limitations as searches for new stable charge particles.

If a signal were found in the stub search at the LHC, it will be difficult to determine the underlying theory. For example, scalar triplets [35, 36, 37, 38, 39, 40, 41], which could be a low-energy remnant of grand unified models that avoid rapid proton decay [42], as well as relaxing constraints from electro-weak precision data, might yield similar signals to fermionic triplets. As with the fermions we considered above, the charged scalar can be seen only when the splitting from the neutral state is close to m_π and triplet's mass is on the order of a few hundred GeV, which provides a sufficient rate for detection. In both cases, the observed signal would be very similar: a charged stub in the central tracker disappearing with no energy deposition in the outer detector.

However, unlike the fermions, scalar triplets can have tree-level couplings with the SM Higgs boson. Generically, these couplings will lead to significant changes in the branching ratio of the neutral Higgs decaying to photons [10]. Measurement of this rate, combined with the observation of stub events, could allow the boson and fermion models to be distinguished.

Anomaly-mediated supersymmetric theories generally contain nearly degenerate neutralinos and charginos. We have seen that the reach at the LHC for such models is greater than 400 GeV for splittings on par with the pion mass, down to ~ 100 GeV neutralinos for splittings around 250 MeV. However since anomaly-mediated spectra tend to have the LSP mass increase with $|\mu|$ while the splitting decreases, natural models of anomaly-mediated supersymmetry will in general not contain an LSP/NLSP pair with small enough splitting to provide a sufficiently large lifetime while also having a small enough mass to be produced copiously at the collider.

Acknowledgements

The authors would like to thank Massimiliano Chiorboli, Beate Heinemann, Dorian Kcira, Greg Landsman, Vladimir Litvine, Maurizio Pierini, Michael Schmitt, Sezen Sekmen, and Maria Spiropulu for their invaluable expertise and advice. LR thanks Caltech for a Moore Fellowship and their hospitality and NYU and the CCPP for its hospitality while some of this work was completed. We would also like to thank the Aspen Center for Physics for providing a simulating and productive environment for discussion and work.

[1] J. Wess and B. Zumino, Nucl. Phys. B **70**, 39 (1974).
[2] N. Arkani-Hamed, S. Dimopoulos and G. R. Dvali, Phys. Rev. D **59**, 086004 (1999) [arXiv:hep-ph/9807344].
[3] L. Randall and R. Sundrum, Phys. Rev. Lett. **83**, 3370 (1999) [arXiv:hep-ph/9905221].
[4] M. Weinstein, Phys. Rev. D **8**, 2511 (1973).
[5] S. Weinberg, Phys. Rev. D **19**, 1277 (1979).
[6] L. Susskind, Phys. Rev. D **20**, 2619 (1979).
[7] T. Moroi and L. Randall, Nucl. Phys. B **570**, 455 (2000) [arXiv:hep-ph/9906527].
[8] M. Cirelli, N. Fornengo and A. Strumia, Nucl. Phys. B **753**, 178 (2006) [arXiv:hep-ph/0512090].
[9] Y. Cui, D. E. Morrissey, D. Poland and L. Randall, JHEP **0905**, 076 (2009) [arXiv:0901.0557 [hep-ph]].
[10] P. Fileviez Perez, H. H. Patel, M. J. Ramsey-Musolf and K. Wang, Phys. Rev. D **79**, 055024 (2009) [arXiv:0811.3957 [hep-ph]].

[11] M. Drees and X. Tata, Phys. Lett. B **252**, 695 (1990).
[12] T. Aaltonen *et al.* [CDF Collaboration], arXiv:0902.1266 [hep-ex].
[13] J. L. Feng, T. Moroi, L. Randall, M. Strassler and S. f. Su, Phys. Rev. Lett. **83**, 1731 (1999) [arXiv:hep-ph/9904250].
[14] J. F. Gunion and S. Mrenna, Phys. Rev. D **62**, 015002 (2000) [arXiv:hep-ph/9906270].
[15] M. Ibe, T. Moroi and T. T. Yanagida, Phys. Lett. B **644**, 355 (2007) [arXiv:hep-ph/0610277].
[16] P. Abreu *et al.* [DELPHI Collaboration], Eur. Phys. J. C **11**, 1 (1999) [arXiv:hep-ex/9903071].
[17] G. Abbiendi *et al.* [OPAL Collaboration], Eur. Phys. J. C **29**, 479 (2003) [arXiv:hep-ex/0210043].
[18] L. Randall and R. Sundrum, Nucl. Phys. B **557**, 79 (1999) [arXiv:hep-th/9810155].
[19] G. F. Giudice, M. A. Luty, H. Murayama and R. Rattazzi, JHEP **9812**, 027 (1998) [arXiv:hep-ph/9810442].
[20] J. Abdallah *et al.* [DELPHI Collaboration], Eur. Phys. J. C **34**, 145 (2004) [arXiv:hep-ex/0403047].
[21] D. Decamp *et al.* [ALEPH Collaboration], Phys. Lett. B **235**, 399 (1990). M. Z. Akrawy *et al.* [OPAL Collaboration], Z. Phys. C **50**, 373 (1991). P. A. Aarnio *et al.* [DELPHI Collaboration], Phys. Lett. B **241**, 425 (1990).
[22] S. D. Thomas and J. D. Wells, Phys. Rev. Lett. **81**, 34 (1998) [arXiv:hep-ph/9804359].
[23] C. H. Chen, M. Drees and J. F. Gunion, Phys. Rev. Lett. **76**, 2002 (1996) [arXiv:hep-ph/9512230].
[24] C. Paus [on behalf of the CMS collaboration], *Prepared for Berkeley Workshop on Physics Opportunities with Early LHC Data, Berkeley, USA, 6-8 May, 2009.*
[25] G. L. Bayatian *et al.* [CMS Collaboration],
[26] G. Aad *et al.* [The ATLAS Collaboration], arXiv:0901.0512 [hep-ex].
[27] W. Adam *et al.* [CMS Trigger and Data Acquisition Group], Eur. Phys. J. C **46**, 605 (2006) [arXiv:hep-ex/0512077].
[28] T. Stelzer and W. F. Long, Comput. Phys. Commun. **81**, 357 (1994) [arXiv:hep-ph/9401258].
[29] T. Sjostrand, S. Mrenna and P. Skands, JHEP **0605**, 026 (2006) [arXiv:hep-ph/0603175].
[30] S. Cucciarelli, M. Konecki, D. Kotlinski and T. Todorov,
[31] A. Djouadi, J. L. Kneur and G. Moultaka, Comput. Phys. Commun. **176**, 426 (2007) [arXiv:hep-ph/0211331].
[32] J. L. Feng and T. Moroi, Phys. Rev. D **61**, 095004 (2000) [arXiv:hep-ph/9907319].
[33] V. M. Abazov *et al.* [D0 Collaboration], Phys. Rev. Lett. **102**, 161802 (2009) [arXiv:0809.4472 [hep-ex]].
[34] A. R. Raklev, arXiv:0908.0315 [hep-ph].
[35] D.A. Ross, M.J.G. Veltman, "Neutral Currents and The Higgs Mechanism," Nucl. Phys. B 95:135,1975.
[36] J. F. Gunion, R. Vega and J. Wudka, Phys. Rev. D **42**, 1673 (1990).
[37] J. R. Forshaw, D. A. Ross and B. E. White, JHEP **0110**, 007 (2001) [arXiv:hep-ph/0107232].
[38] J. R. Forshaw, A. Sabio Vera and B. E. White, JHEP **0306**, 059 (2003) [arXiv:hep-ph/0302256].
[39] M. C. Chen, S. Dawson and T. Krupovnickas, Phys. Rev. D **74**, 035001 (2006) [arXiv:hep-ph/0604102].
[40] P. H. Chankowski, S. Pokorski and J. Wagner, Eur. Phys. J. C **50**, 919 (2007) [arXiv:hep-ph/0605302].
[41] T. Blank and W. Hollik, Nucl. Phys. B **514**, 113 (1998) [arXiv:hep-ph/9703392].
[42] I. Dorsner and P. Fileviez Perez, Nucl. Phys. B **723**, 53 (2005) [arXiv:hep-ph/0504276].